RESEARCH ARTICLE

Reconnaissance Stream Sediments Survey in the Sidakan Vicinity, Iraqi Kurdistan Region

Hawkar A. Abdulhaq[1], Baroz Aziz[2], Varoujan K. Sissakian[3*], Hassan O. Othman[3], Anurag Malik[4]

[1]Department of Civil and Architectural Engineering, School of Science and Engineering, University of Kurdistan Hewler, Erbil, Kurdistan Region-F.R. Iraq
[2]Ministry of Natural Resources, Erbil, Kurdistan Region-F.R. Iraq
[3]Department of Natural Resources Engineering and Management, University of Kurdistan Hewler, Erbil, Kurdistan Region, F. R. Iraq
[4]Regional Research Station, Punjab Agricultural University, Bathinda, Punjab, India

***Corresponding author's email:** f.khajeek@ ukh.edu.krd

Received: 20-08-2020 **Accepted:** 12-11-2020 **Available online:** 31-12-2020

ABSTRACT

A stream survey was conducted in the Sidakan vicinity in the northeastern part of the Iraqi Kurdistan Region, which covered the catchment area of the main stream. The covered area is about 450 km2. The exposed rocks in the study area are mainly igneous with subordinate sedimentary and metamorphic rocks. The catchment area was divided into 14 sub-basins using Global Mapper software. The junction point of the valleys at the end of each sub-basin was sampled. From each junction point, 2 stream sediments were collected. The samples were sieved using the wet method into 2 mm fractions, before the fractions were subjected to x-ray fluorescence (XRF) and x-ray diffraction (XRD) analysis. The results obtained from both tests were used to calculate the concentrations of 9 elements (Cr, Ni, Co, Cu, U, Ag, V, Zn, and Cd). The element concentrations are presented in 9 concentration maps after normalizing the concentration values. Some anomalous results were found. The average concentrations of Ag and Cd were nearly 120 and 266 times higher than the background concentrations (6 mg/kg and 16 mg/ kg, respectively). The acquired data also showed interesting average concentrations for the elements Co, Cr, Ni, and U (280 mg/kg, 999 mg/kg, 375 mg/kg, and 12 mg/kg, respectively). All of these anomalous concentrations are discussed and possible reasons for their existence are given.

Keywords: Stream sediment, Silver, Uranium, Concentration map, Kurdistan, Iraq

1. INTRODUCTION

1.1. General

The mountainous portion of the Iraqi Kurdistan Region has been a conflict network zone for many decades and the political instability has affected the exploration of natural resources. However, the Kurdistan region has recently established projects to exploit hydrocarbon resources.

Access this article online

DOI: 10.25079/ukhjse.v4n2y2020.pp101-118 **E-ISSN:** 2520-7792

Unfortunately, the potential of the mining industry has not been utilized because of the lack of a mineral investment law (Sissakian, 2018). Stream sediments in the catchment area provide an excellent indication of the existing mineralization in exploration studies, and they are important in geochemical prospecting to identify possible sources of anomalous element concentrations (Landry et al., 2014). Sediments in the channels of streams and rivers can contain low levels of metals derived from the weathering of mineralized rocks in the upstream catchment area (Marjoribanks, 2010).

The concentrations of heavy metals can be quite high in stream sediments located close to a deposit, and this is attributed to the weathering processes of mineral deposits. These concentrations decrease with increasing distance from the upstream deposits, except in the first-order stream segments (Fletcher, 1997). Moon and Whateley (2006) suggested that coarse-grain stream-sediment sampling is extremely valuable in areas with poor exposure or in mountainous areas where rock fragments are moved under the force of the gravity. Geochemical studies of the stream sediments have been used by numerous scholars to find minerals of economic interest in the exposed rocks within the catchment areas of streams (Meyer et al., 1979; Plumlee, 1999; Atsuyuki et al., 2005; Marker, 2015). The stream-sediment technique has played a major role in the discovery of many ore bodies around the world. A good example is the discovery of the Panguna porphyry copper/gold deposit on Bougainville Island, Papua New Guinea (Baumer's and Fraser, 1975; Majoribank, 2010).

1.2. Aim

No stream-sediment analysis studies have been conducted in the current study area. Therefore this study is considered as the pioneering one. This study attempts to determine the concentrations of various elements in the region.

1.3. Location

The study area is shown in Fig. 1. It is an area spanning 450 km2. The area is located in the extreme northeastern part of the Iraqi Kurdistan Region along the Iraqi-Iranian international border. The coordinates are [4430521, 4959908], [4430521, 4998885], [4397726, 4998885], and [4397726, 4959908] (UTM WGS 84) (Fig. 1). The only town in the area is Sidakan (25 km northeast of Soran town), with several small villages distributed in the study area. Sidakan can be reached by a paved road from the Erbil–Soran road, but the distant villages are connected with unpaved roads.

2. GEOLOGICAL SETTING

The geological setting of the study area is based on the best available data using the updated geological map and the attached geological report (Sissakian and Fouad, 2014). The geological map of the study area is presented in Fig. 1. The main outcrops in the study area include the Walash (Paleocene–Eocene) and Naopurdan (Paleocene and Oligocene) groups (Sissakian and Fouad, 2014); a detailed geological description of the Walash and Naopurdan groups is presented in the stratigraphy section (4.2). The 3 main components, including the geomorphology, tectonics, and structural geology, as well as the stratigraphy of the study area, are briefly described below.

2.1. Geomorphology

The study area has a mountainous terrain with steep slopes, scarps, and peaks (Fig. 1). The highest peak in the Iraqi Kurdistan Region is known as Halgurd with a height of 3607 m (above sea level [a.s.l.]). It is located in the eastern part of the study area (Fig. 1). However, in the Iraqi Kurdistan Region, the highest peak is located along the Iraqi-Iranian border with a height of 3611 m (a.s.l.), and it is called Cheekha Dar (Google Earth Pro, 2020). Another prominent mountain with a conical peak is located in the southern part of the area and is called the Hassan Bag (Fig. 1), with a height of 2521 m (a.s.l.). The most common geomorphological units in the area, as interpreted from satellite images, are of alluvial origin with 3 recognized features. The first of these are the valley-fill sediments, which fill the main streams and their branches with sediments that range in size from sand (Fig. 2A) to boulders of 1 m or more (Fig. 2B). However, the average size of the sediments range from 2 to 4 mm (Fig. 2A). The second feature is the flood plain sediments. The streams and valleys have narrow courses (Fig. 3A) and steep gradients (Fig. 3B). Therefore, the developed flood plains are very narrow. The top is usually covered by very fine sand and clayey soil. The third of the features are terraces. Two levels of terraces have developed along the streams and main valleys (Fig 3B). The height difference between the 2 levels range from 3 to 5 m, with the first level being 2 to 4 m above the stream base. The pebbles

are of different sizes and lithologies, cemented by calcareous and siliceous cement (Fig. 3B).

2.2. Tectonics and structural geology

The study area is located within the Imbricate zone of the Outer Platform of the Arabian Plate (Fouad, 2012). It is also part of the Zagros fold-thrust belt, which developed within the Zagros foreland basin (Alavi, 2004; Fouad, 2012; Sissakian, 2013). The main tectonic feature in the study area is the Zagros main thrust fault, which is accompanied by other small anticlines and faults. The main features are described below (Sissakian and Fouad, 2012).

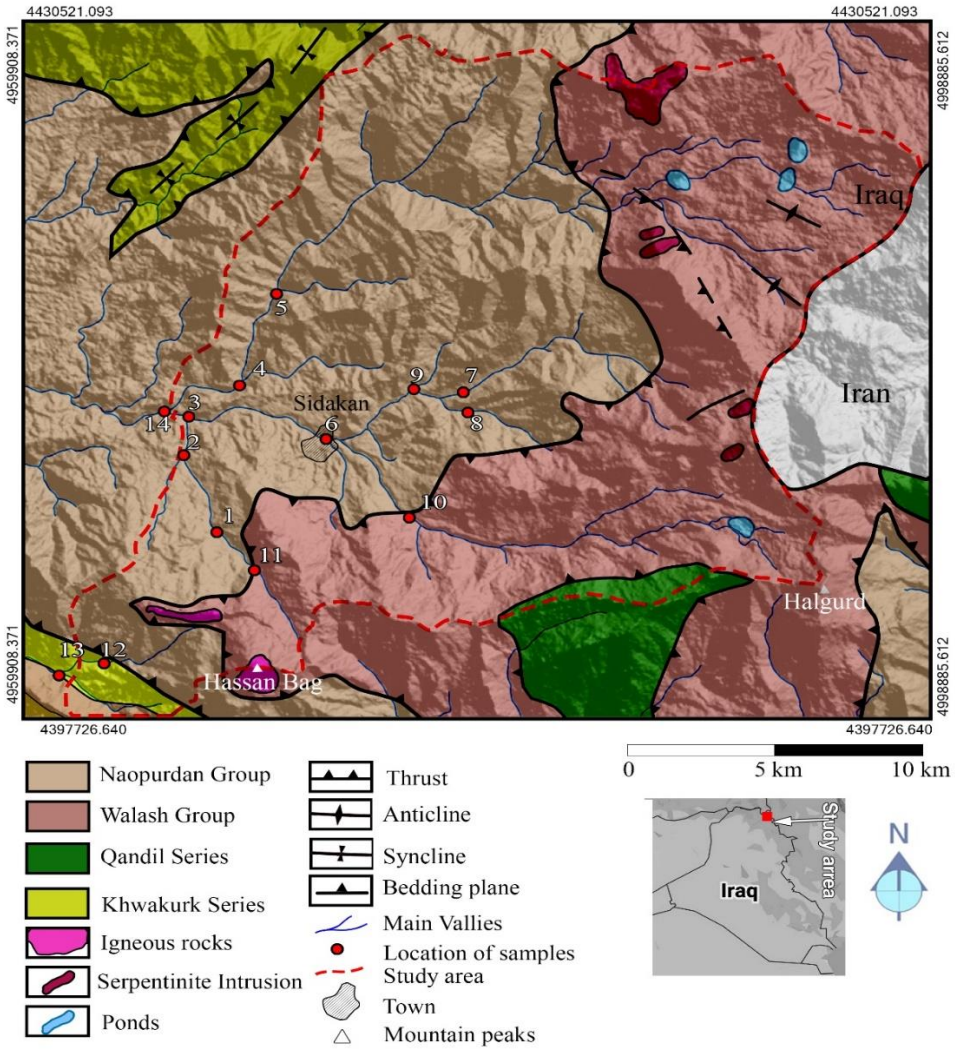

Figure 1. Location and geological map of the study area imposed over a digital terrain map (Aster Global Digital Elevation Model Validation Team, 2009) (according to Sissakian and Fouad, 2014)

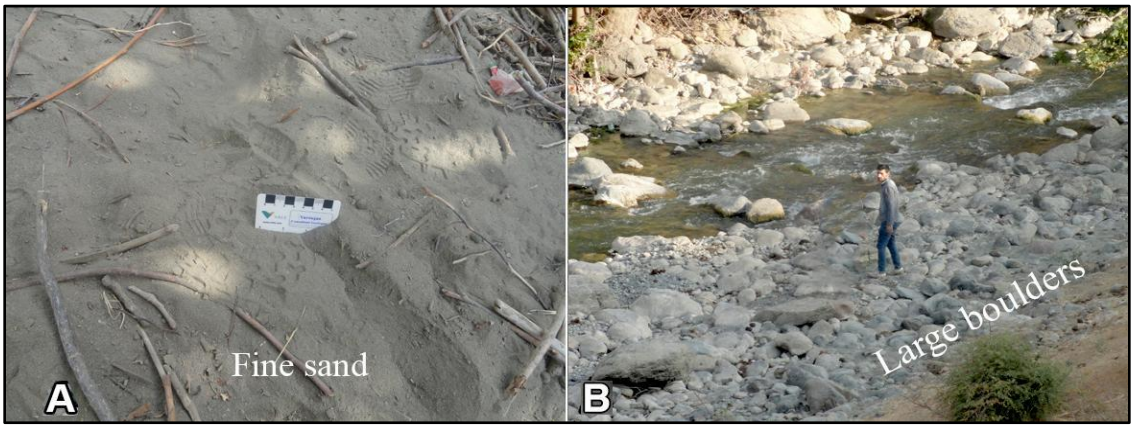

Figure 2. Stream sediments in the study area showing **(A)** fine sand and **(B)** large boulders in the backyard

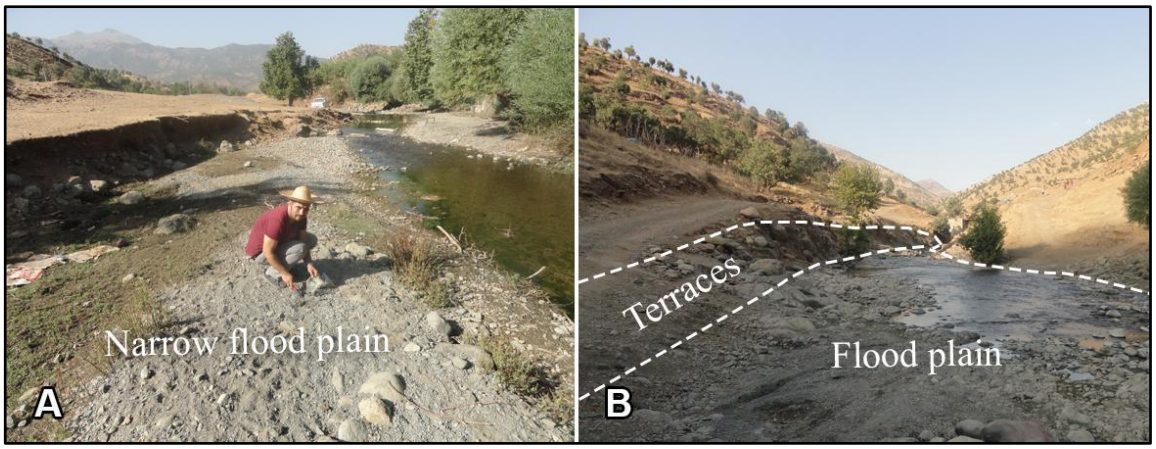

Figure 3. Geomorphological features. **(A)** Developed flood plains showing a narrow flood plain on the left side of the stream. **(B)** Terraces along the stream valley and the steep gradient of the stream

2.2.1. Zagros main thrust fault

The 3 Zagros main thrust faults include 3 sheets that are referred to as the lower, middle, and upper thrust sheets, respectively (Bolton, 1954). Moreover, Bolton (1954) also referred to them as Qandil 1, Qandil 2, and Bulfat thrust massifs. However, only the middle and upper sheets are present in the study area. Bolton (1954) mentioned that the thrust fault mainly has a low angle, although locally, high angle planes were recognized. The middle thrust sheet is characterized by the thrusting of the Qandil Series over the Walash Group, whereas the upper thrust sheet is characterized by the thrusting of the Walash Group over the Naopurdan Group (Fig. 1).

2.2.2. Minor anticlines and faults

Small amplitude folds and many faults exist in the study area and are not more than 5 km in length. They are present in the northeastern part of the study area. All are in the Walash Group (Fig. 1). The different trends, especially of the anticlines, may indicate that their origin is not related to the main tectonic forces, which caused the development of NW–SE trending anticlines. They may have developed as a cause of local deformational forces within the different rock types (sedimentary and

igneous) of the Walash Group (Sissakian and Fouad, 2012).

2.3. Stratigraphy

The following geological units are exposed in the study area (Fig. 1), from the oldest (Qandil Series) to the youngest (Naopurdan Group).

2.3.1. Qandil Series (Cretaceous)

The Qandil Series is exposed on the northeastern side of the study area (Fig. 1) and forms the bulk of the Hasarust Mountain. The Qandil Series consists of sheared limestone (from the sheared zone), phyllites, and massive metamorphosed limestone with some serpentinite intrusions. The thickness of this unit is about 3000 m (Bolton, 1954). The Qandil Series is mainly thrusted over the Walash Group and the Naopurdan Group. On the top of Hassan Bag Mountain, thick exposures of igneous rocks have developed with a sharp contact with the underlying sedimentary and igneous rock sequence of the Walash Group. Ali et al. (2012) mentioned that the rocks are of the Cretaceous age and are represented by ophiolite rocks. However, they did not mention to which rock unit the igneous rocks belong. Based on the study by Sissakian and Fouad (2012), we believe that they belong to the Qandil Series, which are thrusted over the Walash Group east of the Hassan Bag Mountain and Hasarust Range (Fig. 4).

2.3.2. Walash Group (Paleocene–Eocene)

The Walash Group is widely exposed within the study area, especially in the eastern part. The group consists of very thick, mainly basic volcanic sequences, including agglomerate, lava flows, pillow lavas, and ashes with associated dikes. The volcanic rocks are associated with a thick sedimentary sequence, similar to that of the Naopurdan Group, that is composed of thick limestone, red mudstone, and clastics. The thickness of the group in the type locality is 1000 m, but in nearby areas, it is about 3500 m (Stevenson and Cobbett, 1954).

2.3.3. Naopurdan Group (Paleocene- Oligocene)

The Naopurdan Group is widely exposed in the study area, especially in the western part. The group consists of gray shale, coralline limestone, tuffaceous slates, felsic volcanic, basal conglomerate, graywackes, and sandy shale. The stratigraphic position and relation of the group with other formations, beds, and groups are partly obscure. Moreover, the group is considered to interfinger with the Walash Group (Al-Mehaidi, 1974). The thickness of the group in the type locality is about 2000 m, but this thickness is reduced to about 1000 to 1500 m mainly because of thrusting (Stevenson and Cobbett, 1954).

3. MATERIALS AND METHODS

The fieldwork was conducted to achieve the aim of this study and materials such as geological maps of the study area, satellite images, and relevant published papers, which deal with the subject of this study, were used (Ali et al., 2007; Lima et al., 2003). Nylon bags were used to collect the stream-sediment samples. The junctions of the main branches flowing downstream from the main elevated areas and peaks along the main streams were marked manually and considered as sampling points. Two samples were collected from each junction point (each bag contained 1 kg of stream sediment). A total of 14 stream-sediment samples were collected from the junctions of the main streams, representing 14 sub-basins (Fig. 4). However, sub-basin 5 and 10 were divided further into sub-sub-basins, but owing to security issues, we could not reach beyond locations 5 and 10. The stream samples were sieved down to 2 to 4 mm by using a wet sieving method (Moon and Whateley, 2006). The size selection was based on the idea that the potential elements from a nearby source were moved downstream by gravity (Moon and Whateley, 2006). All collected samples were subjected to x-ray fluorescence (XRF) analysis at the University of Kurdistan Hawler, Erbil (Iraqi Kurdistan Region), and 3 samples were subsequently also subjected to x-ray diffraction (XRD) analysis (samples numbers 1, 5, and 10); the XRD analysis was conducted at the Research Center of the Soran University (Iraqi Kurdistan Region). The data acquired from the XRF and XRD

analyses were used to construct the concentration maps (mg/kg) for each detected element and to construct element maps that represent the concentrations in the 2 to 4 mm sieve size samples.

3.1. Sample Collection

The stream-sediment survey was conducted in the vicinity of Sidakan in the Iraqi Kurdistan Region, which is considered an unexplored area. Garrett and Nichol (1967) and Armour-Brown and Nichol (1970) demonstrated that widely spaced stream-sediment sampling for the detection of metallogenic provinces in unexplored regions can be an effective method of delimiting wide-ranging regions of mineral potential. The points of the stream junctions were considered as the sample points for each junction point (Fig. 4); 1 stream-sediment sample was collected for each junction point. However, locally, when the stream sediments were sorted naturally owing to the stream hydraulics, 2 samples were collected from the same point. In total, 14 samples were collected in nylon sacks with each 1 being numbered, well preserved, and packed.

3.2. Concentration Maps Methodology and Characterization

The Global Mapper software was used to map the polygons and drainage net of the sub-basins. The main drainage net was generated in Global Mapper software to navigate the sampling locations (Fig. 4). Adobe Photoshop CC was used for the compilation of the concentration maps of the elements in the samples collected from the study area. To plot the concentration of the elements on the map, we normalized the concentrations of the elements by applying the following formula:

$$EC\ (\%) = (ECx\ /Max)\ *100$$

where EC% is the normalized concentration for each element, which is determined by dividing each element concentration (ECx) by the maximum concentration.

The maps were compiled by coloring the sub-basins with different grades of the same color for each element based on the normalized values. Subsequently, by imposing a cover layer over the grayscale layers, the properties selected for the cover layer were a color code of c7fd00 and the blending mode “color”. Finally, the result was a colorful map from white to dark olive green (Figs. 5–13).

Stream-sediment sampling is one of the most commonly used geochemical exploration methods when surveying an area for its mineral distribution (Eppinger et al., 2003). In our study, samples were collected from active alluvium sediments. Samples were sieved down to a size of 2 to 4 mm by wet sieving in the laboratory. The sieved samples were dried in an oven at a temperature of 65°C for 48 hours followed by grinding of the samples into a homogeneous powder (Moon and Whateley, 2006).

The pulverized samples were pressed into pellets of 5 mm in diameter and their chemical composition were determined using XRF analysis (NEX QC+ QuantEZ Benchtop EDXRF spectrometer, Rigaku, Tokyo, Japan). The result of each element was re-calculated from the mass percentage to mg/kg. A qualitative energy-dispersive x-ray (EDX) measurement was also conducted to confirm the results obtained from the XRF method. The mineralogy of the samples was determined using a Panalytical x-ray diffractometer. The morphology of the powdered samples was determined by scanning electron microscopy. A qualitative EDX measurement was also conducted to confirm the results obtained from XRF.

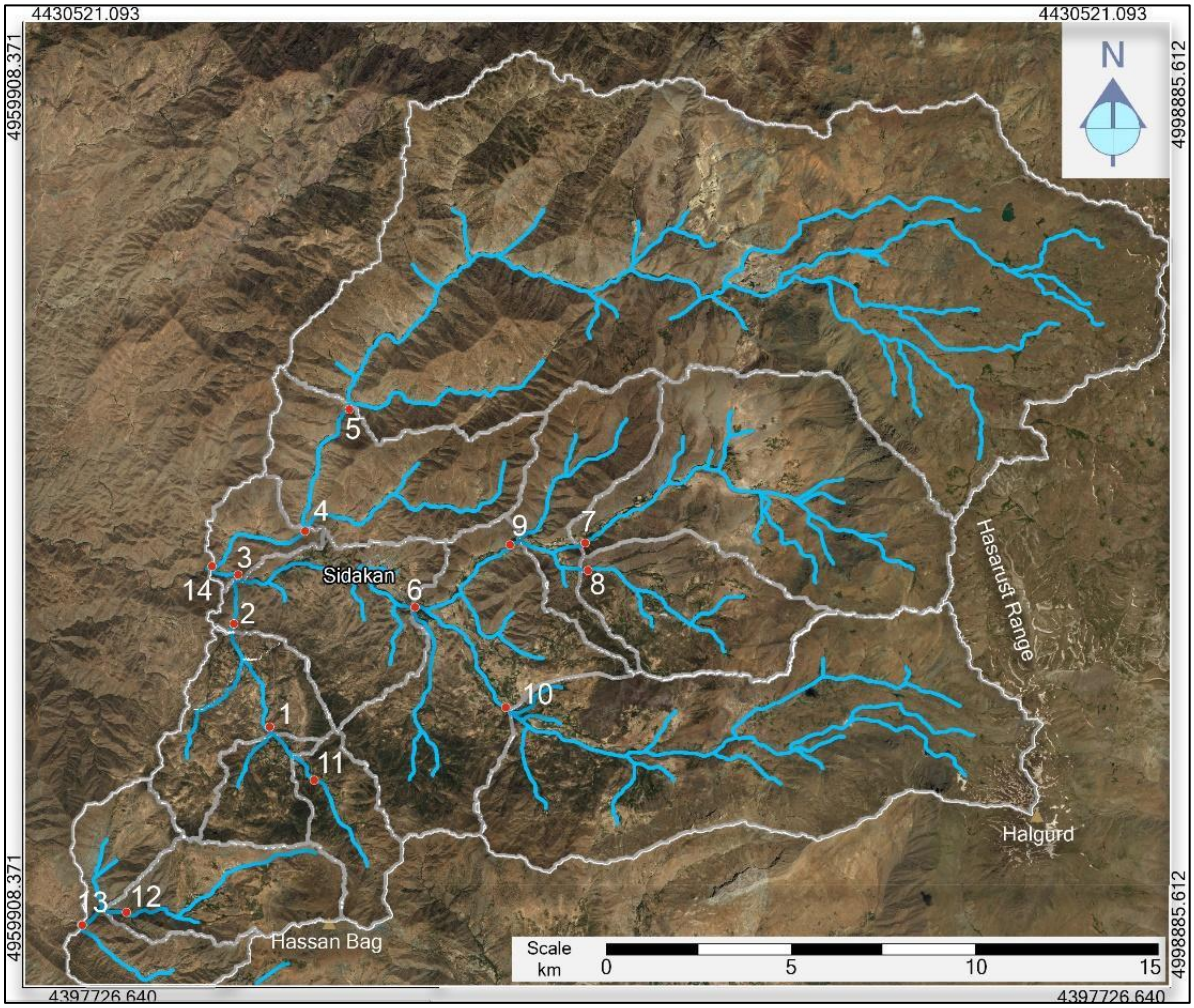

Figure 4. Distribution of the sampling points and sub-basins in the study area (ESRI, 2013)

4. RESULTS

Based on the data acquired during XRF and XRD analysis of the samples, the following results were obtained.

4.1. XRF Method

The chemical composition of the samples acquired from the XRF tests exhibited a large range of diverse elements, including chromium (Cr), copper (Cu), titanium (Ti), cobalt (Co), silver (Ag), uranium (U), cadmium (Cd), and nickel (Ni), which are listed in Table 1. However, only those elements with a significant concentration are presented and interpreted in this study.

The results obtained from XRF analysis showed that there is a high and anomalous concentration of Cr, Cu, and U in the study area. In addition, there are also relatively high concentrations of vanadium (V) and Ni in the samples. However, there are trace concentrations of Ag and U in the samples that exceed the normal concentrations in the crust (Taylor and McLennan, 1995) (Table 1). The qualitative EDX analysis of sample 10 confirms the existence of all the mentioned elements. Correlation factors presented in Table 2 shows the relation between the element co ncentrations.

Table 1: The Concentration (mg/kg) of Major and Trace Elements in the Samples with a Size Fraction of 2 to 4 mm

Sample no.	Cr	Cu	Co	Ag	U	Cd	V	Ni	Pb
1	616	33	182	5	8	18	242	354	ND
2	685	148	286	6	16	24	296	296	ND
3	1680	128	310	8	8	ND	291	635	ND
4	1020	140	274	5	19	17	198	281	ND
5	2040	221	237	ND	23	21	251	286	ND
6	830	124	279	6	5	21	364	261	ND
7	518	19	299	6	7	ND	278	261	ND
8	605	130	204	6	5	23	282	320	ND
9	868	193	310	7	5	ND	309	236	0.003
10	1920	78	283	6	18	18	ND	903	ND
11	426	ND	361	7	7	17	273	184	ND
12	900	85	205	3	5	27	281	401	ND
13	851	208	428	9	18	25	215	343	ND
14	1030	119	260	5	18	18	303	486	ND
Max	2040	221	428	9	23	27	364	903	ND
Min	426	0	182	0	5	0	0	184	ND
Average mg/kg	999	116	280	6	12	16	256	375	NA
Average in the crust mg/kg (Hu and Gao, 2008)	106	27	15	0.05	2.6[a]	0.06	106	34	20[a]

Pb, lead [a]Taylor and McLennan, 1995

Table 2: Correlation Factors between the Concentrations of the Detected Elements in the Samples

Element	Cr	Cu	Co	Ag	U	Cd	V	Ni
Cr	1.00							
Cu	0.57	1.00						
Co	0.28	0.43	1.00					
Ag	0.06	0.27	0.76	1.00				
U	0.67	0.59	0.41	0.06	1.00			
Cd	0.20	0.37	0.14	0.10	0.46	1.00		
V	-0.01	0.41	0.30	0.43	-0.05	0.25	1.00	
Ni	0.76	0.26	0.33	0.38	0.48	0.22	-0.09	1.00

A strong correlation is confirmed by calculating the p value at a significance level of 0.05; a correlation coefficient lower than 0.54 indicates that the elements are not significantly correlated. The results of correlation show strong correlations between elements that might coexist in the same medium (Table 2). There is an interesting correlation (0.76) between Cr and Ni. Because the Walash Group reaches in chromite deposits, existing Ni and Cr deposists in the Walash Group were confirmed by Al-Bassam (2008). Another interesting correlation (0.76) was found between Ag and Co. It is common for Ag to co-occur with Co (Marshal, 2000).

This study aimed to detect the minerals that are present in the study area by conducting a powder XRD analysis of some of the samples. The results indicate the presence of silicates and aluminum silicates such as albite, zeolite, chamosite, Vandendriesscheite, diopside, anorthite, lepidolite, cordierite, and carbonate minerals.

4.2. Spatial Distribution of the Elements

In this section, the spatial distribution of the most probable sources of the detected elements is presented by the created maps. A color code has been used to show the variation in the element concentration in the study area (Figs. 5–13).

4.2.1. Chromium

Elemental Cr spatially appeared in all the collected samples from the study area. The average concentration of Cr was approximately 999 mg/kg and ranged from 426 to 2040 mg/kg. The concentration of Cr in the study area is 9.42 times higher than the concentration of Cr in the crust (Hu and Gao, 2008).

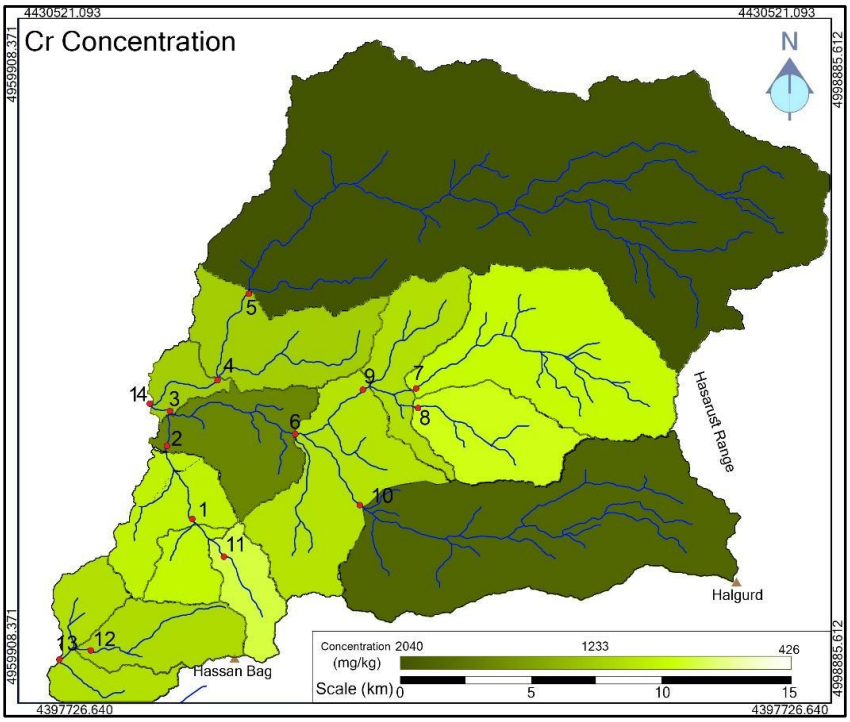

Figure 5. Concentrations of elemental Cr at the various sampling points

4.2.2. Nickel

Elemental Ni appeared in all the collected samples from the study area (Table 1). Both Ni and Cr showed nearly the same concentration patterns over the study area. The average concentration of Ni was approximately 375 mg/kg and ranged from <236 to >903 mg/kg, except in the first-order stream-sediment samples. The highest concentration of Ni was measured in sample number 10 (Fig. 6).

4.2.3. Cobalt

Elemental Co was also detected in all the samples collected from the study area. The average concentration of Co was found to be 280 mg/kg and the highest concentration was 508 mg/kg in sample number 1 (Fig. 7). The sediments derived from the Hassan Bag Mountain showed the highest concentration of the Co element.

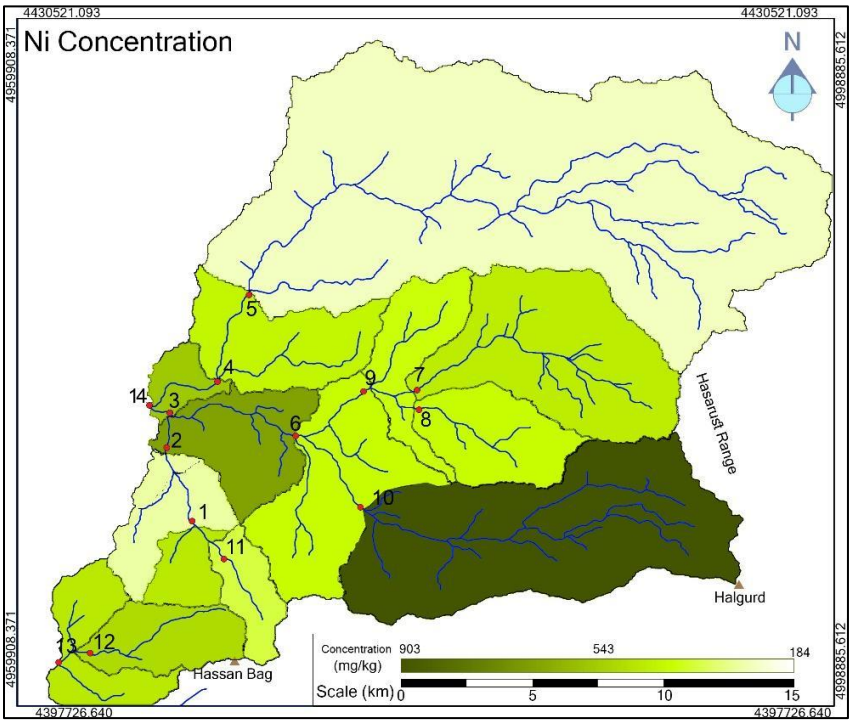

Figure 6. Concentrations of elemental Ni at the various sampling points

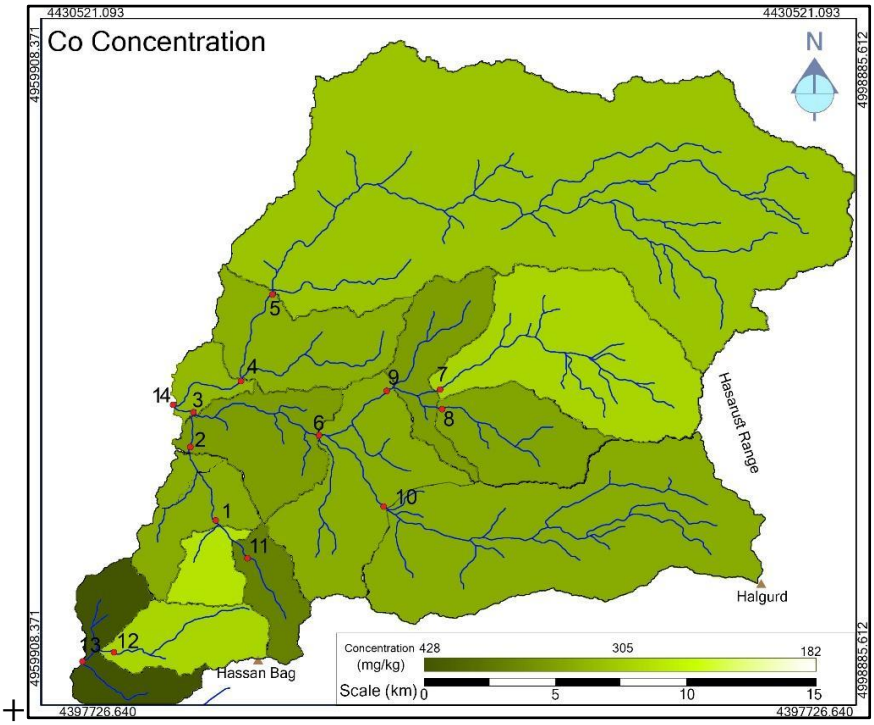

Figure 7. Concentrations of elemental Co at the various sampling points

4.2.4. Copper

The elemental Cu concentration ranged from not detected (ND) to 221 mg/kg (Fig. 8). The highest concentration was measured in sample numbers 5 and 13, which were 201 and 221 mg/kg, respectively. Moreover, it can be observed that Cu was not detected in sample number 11.

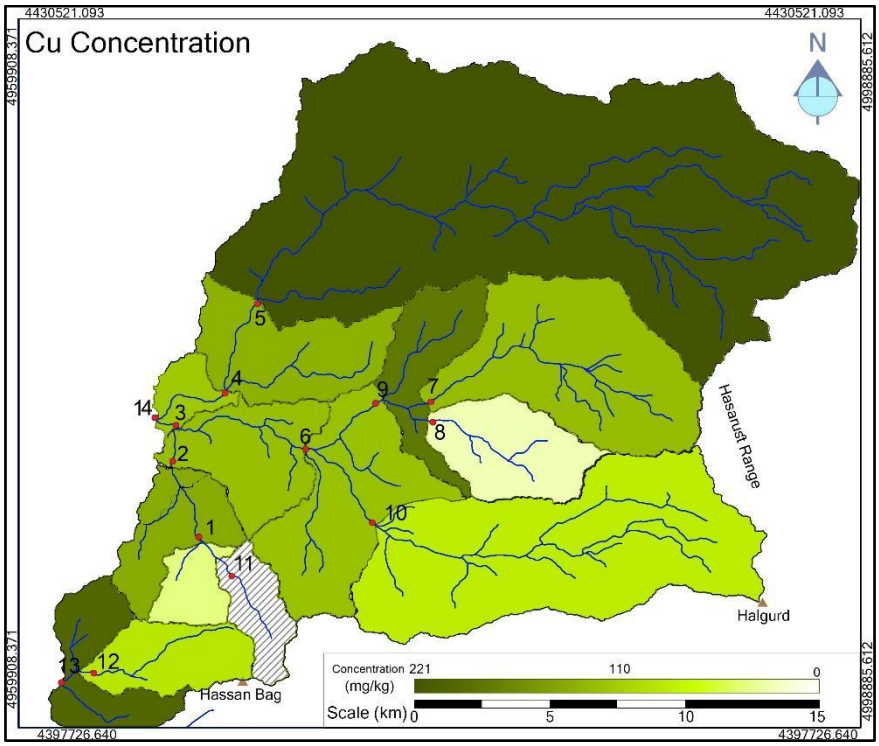

Figure 8. Concentrations of Cu at the various sampling points (the dashed polygon correspond to no detected Cu)

4.2.5. Uranium

Uranium was detected in all of the collected samples from the study area with an average concentration of 12 mg/kg (Table 1). The concertation of U ranged from 5 to 23 mg/kg (Fig. 9).

4.2.6 Silver

The concentration of Ag ranged from not detected to 9 mg/kg (Table 1), with an average of 6 mg/kg, which is 120 times higher than the average Ag concentration in the crust (Taylor and McLennan, 1995). As can be seen from Fig. 10, various concentrations of Ag were detected in different sub-basins; the samples collected in sub-basin numbers 3, 11, and 13 showed anomalous results.

4.2.7 Vanadium

The analysis for the V concentration showed almost the same concentrations in all of the collected samples from the study area. The concentrations of V ranged from ND to 364 mg/kg (Table 1 and Fig. 11). Low concentrations of V were measured in sample number 10, which was derived from the Qandil Series at the Hasarust Mountain.

4.2.8 Cadmium

The Cd concentration ranged from ND to 27 mg/kg with an average of 16 mg/kg, which is approximately 266 times higher than the average Cd concentration in the crust (Hu and Gao, 2008) (Table 1). The highest concentration was measured in the southern part of the Hassan Bag Mountain (Fig. 12).

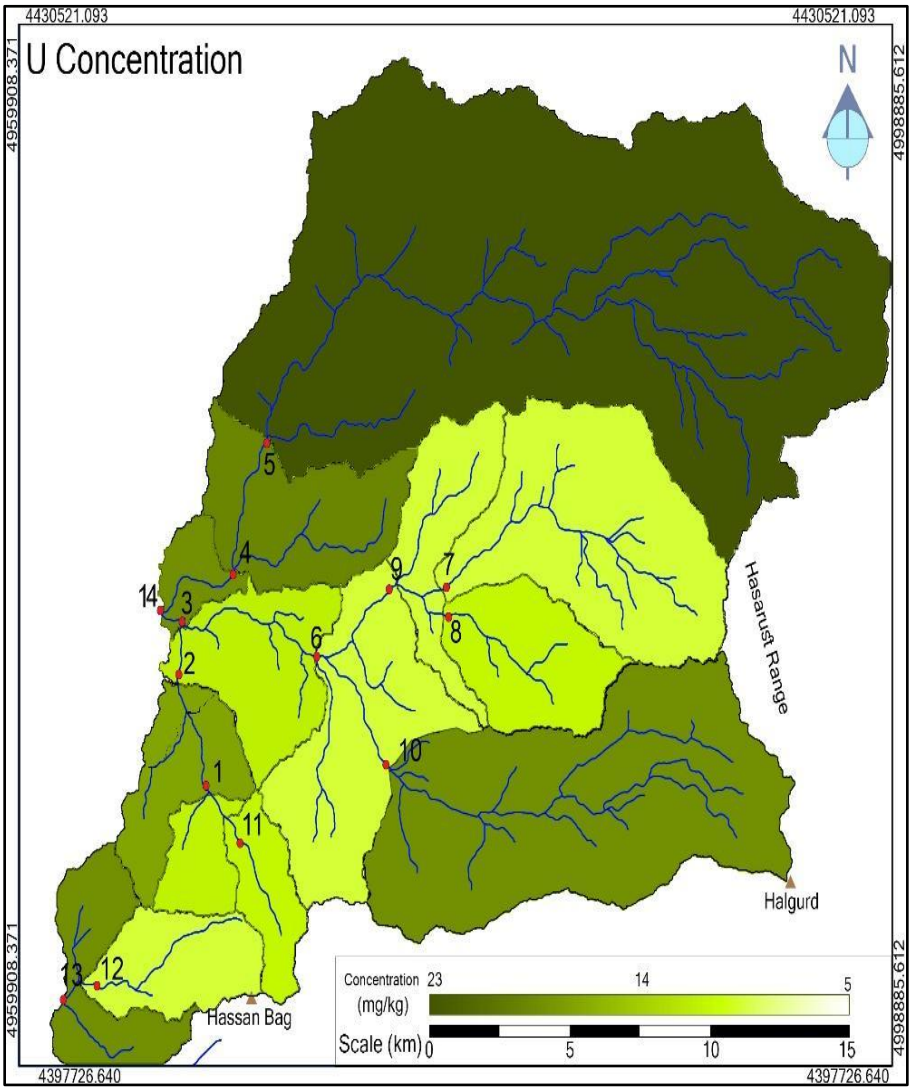

Figure 9. Concentrations of U at the various sampling sites

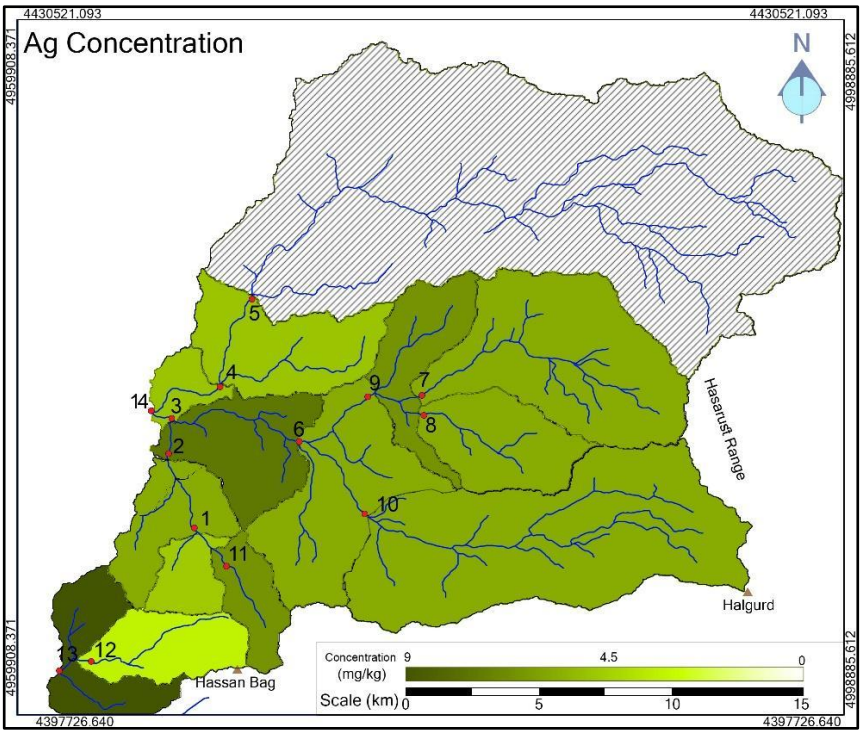

Figure 10. Concentrations of elemental Ag at the various sampling sites (the dashed polygon correspond to areas with no detectable Ag)

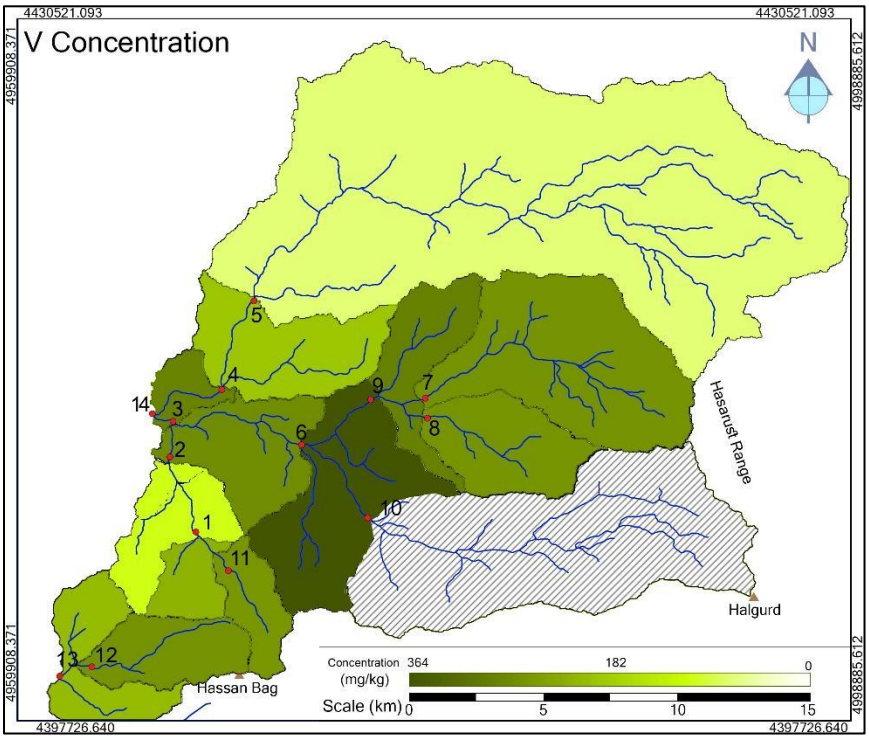

Figure 11. Concentrations of elemental V at the various sampling sites (the dashed polygon correspond to areas with no detectable V)

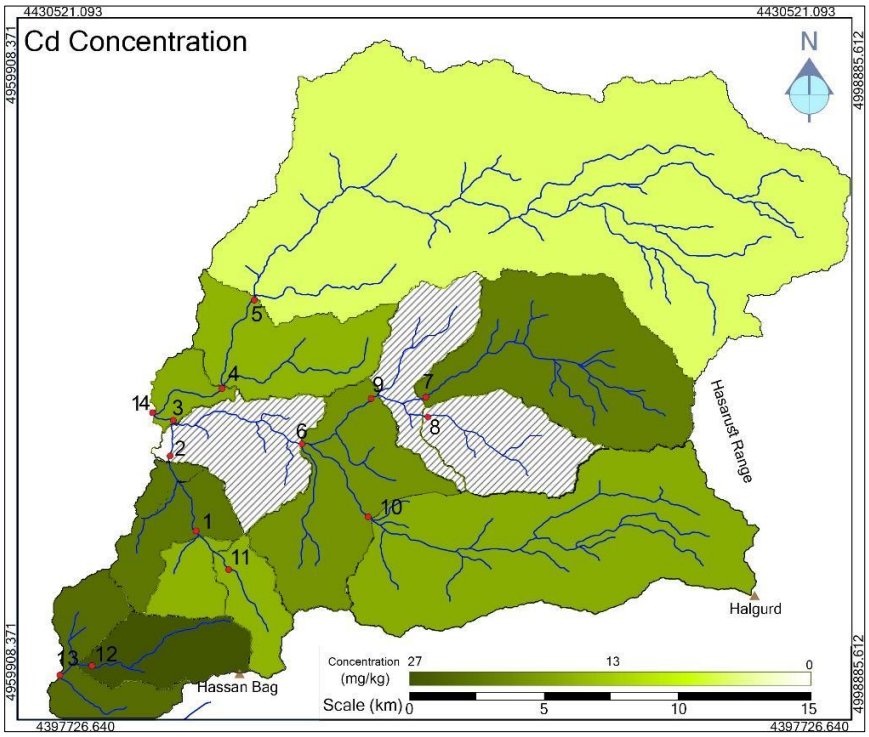

Figure 12. Concentrations of elemental Cd (the dashed polygon correspond to areas with no detectable Cd)

5. DISCUSSION

To indicate the possibility of finding metallic deposits in the exposed rocks within the study area, we compared the average concentrations of the 9 indicated elements in the 14 collected samples with the average concentrations of the elements in the crust, as determined by Hu and Gao (2008) and Taylor and McLennan (1995) (Table 1). We have found that there are several anomalous concentrations when compared with the concentrations of the elements in the crust and basaltic rocks (Fig. 13). Moreover, we found that the average concentration for each of the mentioned elements was higher than those in the crust (Hu and Gao, 2008; Taylor and McLennan, 1995).

Some anomalously high concentrations can be seen for all of the indicated elements, except for Pb, in the sub-basins in the middle part of the study area. These are in sample numbers 2, 3, 4, and 6 and can be attributed to (1) the exposed rocks in the concerned sub-basins that contain higher concentrations of the elements than those exposed at the rims of the main basin, (2) the presence of fine tributaries that are not present in the topographic map and therefore the limits of the sub-basin are not accurately indicated, or (3) the presence of topographic obstacles in the streams which caused more dumping of the stream sediments than the other streams with normal gradients.

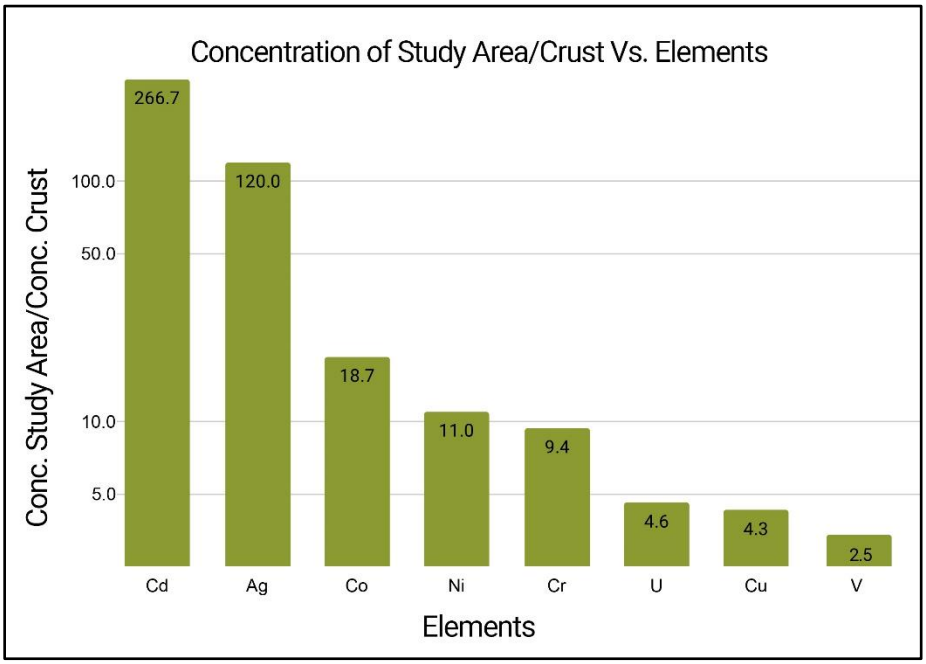

Figure 13. The ratio of the average concertations of the elements measure for the study area and the concentration of the elements in the crust (the vertical scale is a logarithmic scale)

The concentration of Cr was highest in sample numbers 5 and 10 (Fig. 5), and this can be attributed to both samples (5 and 10) being driven along from the upstream serpentine intrusions (Fig.1). Existing in these serpentine intrusions is the main reason that could explain the higher concentration of Cr in these 2 samples as mentioned by Pearre and Van Heyl (1960). The concentration of Ni was measured to be nearly 5 times higher than the concentration of Ni in the crust (Hu and Gao, 2008), and the Ni concentration in the study area was 4.5 times higher than the concentration of Ni in igneous rock (Wells, 1943). The highest concentration of Ni is in sample number 10 (903 mg/kg) where, upstream of this sub-basin, the rocks are derived from the Qandil Series (Fig. 1). In addition, there is a strong correlation between the Cr and Ni concentrations (correlation coefficient of 0.76) (Table 2), which is indicative that both elements coexisted in the study area and that both could be derived from serpentinite that is rich in Cr and Ni. There are, thus, 2 possible reasons for the coexistence of Cr and Ni: first, 1 of the major outcrops of the study area is the Walash Group, which is rich in Ni and Cr (Al-Bassam, 2008), and second, serpentinite is found in the study area (Morrison et al., 2015 and Pędziwiatr et al., 2018).

The concentration of Co is higher in the Hassan Bag-related sub-basins (No. 11 and 13) because the exposed rocks of the Hassan Bag contain calk-alkaline basalt rocks (Ali et al., 2012). In general, the average concentration of Co in the study area is 2.4 times higher than the average concentration of Co in the igneous and metamorphic rocks such as dunite and serpentinite (Schulz, 2018). The concentration of Cu shows nearly the same trends as observed for the concentration of Co, except in sample number 5, which showed a significantly higher concentration (221 mg/kg). The average concentration of Cu (116 mg/kg) in the study area is nearly the same concentration as Cu in the Basaltic rocks (Hu and Gao, 2008). The main reason for the higher concentration in sample number 5 is because of the presence of several serpentine intrusions in the sub-basin where sample 5 was collected. Similar cases have been discussed by other authors (Saglam, 2017; Shallari et al., 1998).

Another interesting result is the concentration of U. The detected concentration was considered to be a significant value when compared with the average concentration of U in the crust, which is only 2 mg/kg (Pękala et al., 2017). The XRD results suggest the presence of Vandendriesscheite, which is a U and Pb containing mineral, which could explain the relatively high concentration of U in the collected samples. However, Pb was only detected in sample number 9 and the concentration of Pb in sample number 9 was 0.003 mg/kg. Additionally, there is a significant correlation between U and Cr (correlation coefficient 0.67) (Table 2). The possible reason for the coexistence of U and Cr is the composition of the Walash Group, which contains both U and Cr (Aswad et al., 2014).

The concentration of Ag in the study area is nearly 120 times higher than the average concentration of Ag in the crust (Taylor and McLennan, 1995) (Fig. 13). We believe that there is Ag enrichment in the rocks of Hassan Bag (alkaline basic rock). Such enrichments have been mentioned previously by Boyle (1968). Moreover, he mentioned that most of the silver is found in sulfides and ferromagnesian minerals and, therefore, the basic rocks will contain higher concentrations of silver. This is another explanation for the anomalous concentrations measured in sub-basins numbers 3, 11, and 13 in which the stream sediments are derived from the basic rocks that are exposed in the Hassan Bag Mountain.

The high concentration of Cd in some of the samples is most probably related to the mafic rocks, which are exposed in Hassan Bag Mountain. Dostal and Elsonu (1979) mentioned that mafic rocks usually contain high Cd concentrations.

Vanadium can be found in most of the rocks of the earth's crust, but the highest concentrations are found in ultrabasic and basic rocks, which is about 200 mg/kg (Aubert and Pinta, 1980). The concentration of V in the study area was 2.8 times higher than the concentration of V in basic and ultrabasic rocks. This can be attributed to the exposed mafic alkaline igneous rocks at the Hassan Bag Mountain. The high concentration of V in these types of rocks was determined by McCormick (1978).

Based on the results obtained from XRF and XRD analysis of the collected samples, which showed high and anomalous concentrations, we highly recommend further studies to conduct systematic geochemical exploration with detailed geological mapping.

6. CONCLUSIONS

The reconnaissance survey of the stream sediments in the study area revealed significant concentrations of some elements. This was determined by studying 14 samples collected from 14 sub-basins. The collected stream samples were subjected to XRF analysis and 4 of the samples were further subject to XRD analysis as well. The results obtained from XRF analysis showed that the average concentrations of Ag and Cd are 6 mg/kg and 16 mg/kg, respectively, indicating that the concentration of Ag is 80 times higher than the Ag concentration in the crust. We believe that the reason for this high anomalous result can be attributed to the exposed basic igneous rocks at the Hassan Bag Mountain. The anomalous samples are located in the sub-basins that drain from the mentioned mountain.

Additional high anomalous results were determined for the average concentrations of Co and Cr (280 mg/kg and 999 mg/kg, respectively). The average concentration of Co and Cr is 25 and 9 times higher than those in the crust, respectively. The higher values can be attributed to the exposed serpentinized bodies in the related sub-basins, in addition to the exposed igneous rocks within the Qandil Series.

The XRF results of the collected stream samples also showed anomalous concentrations for the remaining elements (Ni, V, Zn, and U), which were most probably derived from the exposed igneous rocks in the study area. The differences in the concentrations can be attributed to the concentrations of the mentioned elements in the parent rocks, the size of the sub-b asin, and the remoteness of the exposed igneous rocks of the sampled locations.

However, the indicated Cu concentrations in the collected samples were low when compared with those of other elements. Among the 14 collected samples, 3 of them showed concentrations that were lower than the average concentration in the crust, which is 55 mg/kg, whereas the average concentration in the collected samples was 116 mg/kg. The results for Pb (not detected in the samples) remain unclear. However, unintentional analytical errors cannot be ignored, not only for the Cu and Pb measurements but also for all the other elements in the samples.

It is worth mentioning that the results of the current reconnaissance stream survey do not indicate the presence of concentrations of elements with economic potential. Nevertheless, more detailed sampling of those sub-basins that showed anomalous results may give different results than those presented in this study.

ACKNOWLEDGMENTS

The authors would like to express their sincere gratitude to Dr Prof Mádai Ferenc from the University of Miskolc, Hungary, for his critical review of the manuscript, which enhanced the current article. Furthermore, thanks to Mr. Alan Colin for reviewing the linguistics.

REFERENCES

Abdolmaleki, M., Mokhtari, A. R., Akbar, S., Alipour-Asll, M., & Carranza, E. J. M. (2014). Catchment basin analysis of stream sediment geochemical data: Incorporation of slope effect. *Journal of Geochemical Exploration*, 140, 96-103.

Alavi, M. (2004). Regional stratigraphy of the Zagros fold-thrust belt of Iran and its proforeland evolution. *American Journal of Science*, 304(1), 1-20.

Al-Bassam, K. S. (2013). Mineral resources of Kurdistan region, Iraq. *Iraqi Bulletin of Geology and Mining,* 9(3), 103-127.

Ali, K., Cheng, Q., Li, W., and Chen, Y. (2006). Multi-element association analysis of stream sediment geochemistry data for predicting gold deposits in south-central Yunnan Province, China. *Geochemistry Exploration, Environment, Analysis*, 6(4), 341-348.

Ali, S. A., Buckman, S., Aswad, K. J., Jones, B. G., Ismail, S. A., & Nutman, A. P. (2012). Recognition of Late Cretaceous Hasanbag ophiolite-arc rocks in the Kurdistan Region of the Iraqi Zagros suture zone: A missing link in the paleogeography of the closing Neotethys Ocean. *Lithosphere,* 4(5), 395-410.

Al-Mehaidi, H.M. (1974). Geological investigation of Mawat- Chwarta area, NE Iraq. Iraq Geological Survey Library Internal Report No. 609.

Armour-Brown, A., and Nichol, I. (1970). Regional geochemical reconnaissance and the location of metallogenic provinces. *Economic Geology*, 65(3), 312-330.

ASTER Global Digital Elevation Map Announcement (2009). NASSA, Jet Propulsion Laboratory. https://asterweb.jpl.nasa.gov/gdem.asp.

Aswad, K.J., Al-Samman, A.H., Aziz, N.R. and Koyi, A.M. (2014). The geochronology and petrogenesis of Walash volcanic rocks, Mawat nappes: constraints on the evolution of the northwestern Zagros suture zone, Kurdistan Region, Iraq. *Arabian Journal of Geosciences*, 7(4), 1403-1432.

Aubert, H. and Pinta, M. (1980). Trace Elements. In: Soils. 1st ed. Burlington: Elsevier.

Baumer, A., & Fraser, R. B. (1975). Panguna porphyry copper deposit, Papua New Guinea. Economic geology of Australia and Papua New Guinea I–Metals. Australasian Institute of Mining and Metallurgy, Melbourne, 855-866.

Bolton, C.M.G. (1954). Geological Map of Kurdistan Series, scale 1:100 000, sheet K6, Halabcha. Iraq Geological Survey Library Internal Report No.278.

Boyle, R.W. (1968). Geochemistry of silver and its deposit notes on geochemical prospecting for the element. Geological Survey of Canada. Ottawa, Ont: Canada, *Department of Energy, Mines and Resources,* 160, l-96.

Dostal, J., Elson, C., & Dupuy, C. (1979). Distribution of lead, silver and cadmium in some igneous rocks and their constituent minerals. *The Canadian Mineralogist,* 17(3), 561-567.

Eppinger, R. G., Briggs, P. H., Rieffenberger, B., Dorn, C. V., Brown, Z. A., Crock, J. G., ... & Wilson, S. A. (2003). Geochemical data for stream sediment and surface water samples from Panther Creek, the Middle Fork of the Salmon River, and the Main Salmon River, collected before and after the Clear Creek, Little Pistol, and Shellrock wildfires of 2000 in central Idaho (pp. 1-32). US Department of the Interior, US Geological Survey.

ESSRI (2013). ArcGIS REST Services Directory. World Imagery. https://services.arcgisonline.com/ArcGIS/rest/services/World_Imagery/MapServer/0.

Fletcher, W.K. (1997) Stream sediment geochemistry in today's exploration world. In: Proceedings of exploration, Vol 97, pp. 249-260.

Fouad, S.F. (2012). Tectonic Map of Iraq, scale 1: 1000000, 3rd edition. Iraq Geological Survey Publications, Baghdad. Iraq.

Garrett, R. G. (1966). Regional geochemical reconnaissance of eastern Sierra Leone. Ph.D. Thesis, Vol 1. http://hdl.handle.net/10044/1/17705

Hu, Z. and Gao, S. (2008). Upper crustal abundances of trace elements: a revision and update. *Chemical Geology,* 253(3-4), 205-221.

Lahermo, P., Väänänen, P., Tarvainen, T., & Salminen, R. (1996). Geochemical atlas of Finland, part 3: Environmental geochemistry–stream waters and sediments. Geological Survey of Finland, Espoo.

Landry, S. T., Sylvestre, G., Djibril, K. N. G., Timoleon, N., Boniface, K., & Paul, N. J. (2014). Stream sediment geochemical survey of Gouap-Nkollo prospect, southern Cameroon: implications for gold

and LREE exploration. *American Journal of Mining and Metallurgy*, 2(1), 8-16.

Lima, A., De Vivo, B., Cicchella, D., Cortini, M., & Albanese, S. (2003). Multifractal IDW interpolation and fractal filtering method in environmental studies: an application on regional stream sediments of (Italy), Campania region. *Applied Geochemistry,* 18(12), 1853-1865.

Marjoribanks, R. (2010). Geological methods in mineral exploration and mining. Springer Science & Business Media.

McCormick, G. R. (1978). Vanadium-titanium-bearing mixed-layered clay from Potash Sulphur Springs, Arkansas. *Clays and Clay Minerals*, 26(2), 93-100.

Akintola, A. I., Bankole, S. I., Ikhane, P. R., & Salami, O. O. (2014). Geology and geochemical analysis of stream sediments and soil samples of Ijero Ekiti and its environs southwestern Nigeria. *Advances in Environmental Biology*, 1:68-87.

Marshall, D., & WATKINSON, D. H. (2000). The Cobalt mining district: Silver sources, transport and deposition. *Exploration and Mining Geology,* 9(2), 81-90.

Meyer, W. T., Theobald, PK, Jr., Bloom, H. (1963). Stream Sediment Geochemistry. In: Geophysics and Geochemistry in the Search for Metallic Ores; Peter J. Hood, editor; Geological Survey of Canada, Economic Geology Report 31, p. 411-434, 1979. Economic Geology Report, (31), 411.

Moon, C. J., Whateley, M. K., & Evans, A. M. (2006). Introduction to mineral exploration, 2nd edition. Blackwell Publishing.

Morrison, J.M., Goldhaber, M.B., Mills, C.T., Breit, G.N., Hooper, R.L., Holloway, J.M., Diehl, S.F. and Ranville, J.F. (2015). Weathering and transport of chromium and nickel from serpentinite in the Coast Range ophiolite to the Sacramento Valley, California, USA. *Applied Geochemistry*, 61:72-86.

Ohta, A., Imai, N., Terashima, S., & Tachibana, Y. (2005). Influence of surface geology and mineral deposits on the spatial distributions of elemental concentrations in the stream sediments of Hokkaido, Japan. *Journal of Geochemical Exploration,* 86(2), 86-103.

Pędziwiatr, A., Kierczak, J., Waroszewski, J., Ratié, G., Quantin, C. and Ponzevera, E. (2018). Rock-type control of Ni, Cr, and Co phytoavailability in ultramafic soils. *Plant and Soil,* 423(1-2), 339-362.

Pękala, A. (2017,). Thorium and Uranium in the Rock Raw Materials Used For the Production of Building Materials. In IOP Conference Series: Materials Science and Engineering, 245(2):022033.

Pearre, N. C., & Van Heyl, A. (1960). Chromite and other mineral deposits in serpentine rocks of the Piedmont Upland, Maryland, Pennsylvania and Delaware (No. 1082). US Government Printing Office.

Plumlee, G. S. (1999). The environmental geology of mineral deposits. Society of Economic Geologists. *Reviews in Economic Geology,* 6 A:71-116.

Robb, L. (2013). Introduction to ore-forming processes. John Wiley & Sons.

Saglam, C. (2017). Heavy metal concentrations in serpentine soils and plants from Kizildag national park (Isparta) in Turkey. *Fresenius Environmental Bulletin,* 26(6), 3995-4003

Schulz, K. J., DeYoung, J. H., Seal, R. R., & Bradley, D. C. (Eds.). (2018). Critical Mineral Resources of the United States: Economic and Environmental Geology and Prospects for Future Supply. USGS. Professional Paper 1802. DOI:10.3133/pp1802

Shallari, S., Schwartz, C., Hasko, A. and Morel, J.L. (1998). Heavy metals in soils and plants of serpentine and industrial sites of Albania. *Science of the Total Environment,* 209(2-3), 133-142.

Sissakian, V. K. (2013). Geological evolution of the Iraqi Mesopotamia Foredeep, inner platform and near surroundings of the Arabian Plate. *Journal of Asian Earth Sciences*, 72, 152-163.

Sissakian, V.K. (2018). Minerals Wealth in Kurdistan. A Critical Review. UKHJSE, Vol. 2, No. 2, p. 23 – 36.

Sissakian, V. K., and Fouad, S. F. (2012). Geological Map of Iraq, scale 1: 1000000, 4th edition. Iraq Geological Survey Publications, Baghdad, Iraq.

Sissakian and Fouad. (2014). Geological Map of Erbil and Mahabad Quadrangles, scale 1:250000, 2nd edition. Iraq Geological Survey Publications, Baghdad, Iraq.

Stevenson, P.C. and Cobbett, G.P.R. (1954). Geological Map of Kurdistan Series, scale 1:100 000, sheet K3, Merga Sur. Iraq Geological Survey Library Internal Report No.275.

Taylor, S.R. and McLennan, S.M. (1995). The geochemical evolution of the continental crust. *Reviews of Geophysics*, 33(2), 241-265.

Wells, R. C. (1943). Relative abundance of nickel in the earth's crust. Professional Paper, 205-A. DOI: 10.3133/pp205A.